Statistical properties of the heat flux between two nonequilibrium steady-state thermostats

Mona Lameche and Antoine Naert*
Université de Lyon, ENS de Lyon, CNRS, Laboratoire de Physique, F-69342 Lyon, France

(Received 23 April 2020; revised 21 January 2021; accepted 9 March 2021; published 29 April 2021)

We address the question of transport of heat in out-of-equilibrium systems. The experimental setup consists in two coupled granular gas nonequilibrium steady-state (NESS) heat baths, in which Brownian-like rotors are imbedded. These rotors are electromechanically coupled, thanks to DC micromotors, through a resistor R such that energy flows between them. The average flux depends linearly in the difference in the baths' temperature. Varying R allows extrapolation in the nondissipative coupling limit ($R \to 0$). We show that in this limit the heat flux obeys the fluctuation theorem in a form proposed by Jarzynski and Wójcik in 2004 [C. Jarzynski and D. K. Wójcik, Phys. Rev. Lett. **92**, 230602 (2004)] for the fluctuations of the flux between finite size equilibrium heat baths.

DOI: 10.1103/PhysRevE.103.042143

I. INTRODUCTION

In dissipative systems, nonequilibrium steady states (NESS) result from the balance, in the average, between the work supplied and the heat dissipated per time unit. (See, for instance, turbulent flows, granular gases, etc.) In many physical systems of interest, work is injected from the boundaries as dissipation occurs in the bulk. One of the simplest experimental setups one can think of to investigate the energy transport in NESS systems is two granular gas thermostats, at distinct effective temperatures, weakly coupled to one another. Both are designed completely alike but kept in steady states by separate external forcings (periodic vertical acceleration). In such granular gas heat baths, the stationary random motion of the beads resulting from the external power supply mimics thermal agitation, characterized by an effective temperature. The mean kinetic energy of the beads is sometimes called "granular temperature" [1]. It is our working hypothesis that the effective temperatures, measured by different means, play the same role as equilibrium temperatures [2,3], in a sense to be discussed below.

Let us briefly focus on the granular gas itself. (For reviews, see Refs. [4,5], for example.) The random motion of the inelastic beads is the result of a complex process in which mechanical power is injected at the bottom and dissipated into heat by collisions and viscous drag. The "effective temperature" differs from the "equilibrium temperature" in the sense that the former takes into account only a very reduced number of degrees of freedom, at macroscopic scale, averaging out small scales degrees of freedom. As a result, the values of the effective temperature are definitely distinct. The energy per time unit needed to sustain motion is ultimately completely dissipated into heat. It is the so-called "housekeeping heat" [6] for the granular gas. However, the system of interest here is not the granular gas but a rotor immersed into it, the former being merely used as a heat bath, causing random forcing on the rotor.

This model experiment is implemented to investigate specifically the fluctuations of the energy flux $\phi(t)$ between two NESS thermostats kept at distinct effective temperatures kT_i $(i = 1; 2)$. Working on a macroscopic scale setup allows one to measure conveniently $\phi(t)$ between the baths and the temperature in each at the same time. We write the temperature kT_i in energy units (J), as usual in statistical physics. The Boltzmann constant k_B might be used to make a conversion into the Kelvin temperature scale, a conversion not necessary in general. We opt for writing kT_i without specifying separately k and T. First, we have a linear dependance of the mean heat flux in the temperature difference: $\overline{\phi} \propto kT_1 - kT_2$. That is the Fourier law for heat conduction [7]. Second, the statistics of $\phi(t)$ are examined in terms of the fluctuation theorem. Indeed, as the flux is an irreversible transport process between the baths when $kT_1 \neq kT_2$, it causes an asymmetry that can be regarded in these terms.

Let us briefly introduce the fluctuation theorem (FT), which is a cornerstone of the so-called stochastic thermodynamics. The FT refers to a set of theoretical results obtained in several steps in the 1990s [8–11]. It compares the probability of seeing the entropy of a dynamical or stochastic system increase or decrease, when forced off equilibrium by an external perturbation, with respect to a heat reservoir. It explains in a very primal expression the irreversibility of a dynamical process:

$$\frac{P(\sigma_\tau)}{P(-\sigma_\tau)} = \exp(\sigma_\tau), \quad \text{for } \tau \to \infty. \tag{1}$$

P is the probability of σ_τ, the entropy rate $\sigma = dS/dt$ averaged over a (large) time window τ. The FT is often referred to as the most general expression of the second principle. Detailed reviews on these important theoretical advances can be found in Refs. [12,13]. Experimental access to observables related to entropy fluctuations often requires systems at the

*Antoine.Naert@ens-lyon.fr

micrometer scale so that molecular thermal fluctuations do not average out. Due to technical difficulties, experimental contributions mostly appeared later. (See a review in [14,15].) We note, however, that some early experiments were performed at macroscopic scale [16].

The entropy being generally unmeasurable, the relation $dS = \beta dE$ is used to express the FT for observables such as energy, and the bath's inverse temperature is $\beta = \frac{1}{kT}$. It is worth noting that although the FT holds for the system as far as desired from equilibrium, the heat reservoir mentioned above is always implicitly at equilibrium and in the thermodynamic limit, as traditionally assumed in the canonical formalism of statistical mechanics [17].

Now, consider that the system, instead of being subject to a deterministic forcing, is perturbed by the coupling with another thermostat. The result is then a net transfer of energy from one thermostat to the other, and the FT should still apply. Indeed, one intuitively expects the back-and-forth fluxes (negative and positive realizations of ϕ) to obey the FT. Indeed, each system i in contact with a heat bath at kT_i exchanges energy with the other one at a different temperature. We measure $\phi(t)$, the instant resulting energy flux from one to the other, and vice versa. The time coarse-grained flux is $\phi_\tau(t) = \frac{1}{\tau}\int_{t-\frac{\tau}{2}}^{t+\frac{\tau}{2}} \phi(t-t')dt'$. The FT is then, for large τ,

$$\frac{P(\phi_\tau)}{P(-\phi_\tau)} = \exp(\mu\tau\phi_\tau). \tag{2}$$

The exponent μ is the only free parameter. Jarzynski and Wójcik proposed in 2004 the exchange fluctuation theorem (XFT) for heat flux between two equilibrium heat baths [18]. According to these authors, the prefactor μ in Eq. (2) is nothing but the inverse temperature difference: $\mu = \beta_1 - \beta_2 = \frac{1}{kT_1} - \frac{1}{kT_2}$.

The heat transport has been investigated in terms of the XFT in the past, numerically and experimentally for different kinds of coupling [19–21], and theoretically for non-Gaussian baths [22]. In a previous experimental study, we made use of a similar granular gas experiment to investigate the energy transport between NESS heat baths, weakly coupled by electromechanical devices. Equation (2) was shown to hold precisely; however, a quantitative departure from the XFD was observed, as the exponent μ was significantly distinct from $\Delta\beta$ [7]. No explanation was provided at the time. One could invoke the out-of-equilibrium character of the heat baths themselves, but the dissipative nature of the coupling could also be at play (an Ohmic resistance in the electric circuit).

In the present study we investigate experimentally the bias due to the dissipative coupling. We show that the XFT is recovered quantitatively in the nondissipative limit, i.e., $\mu \to \Delta\beta$, for vanishing resistance. We stress the specific feature that the heat baths are in NESS and not in equilibrium states, as implicitly assumed in [18].

The experimental setup is presented in the next section. In Sec. III the measurement principle of the energy flux and temperatures is explained. In Sec. IV the test of the XFT is presented in the nondissipative coupling limit, followed by a short discussion of the results in Sec. V.

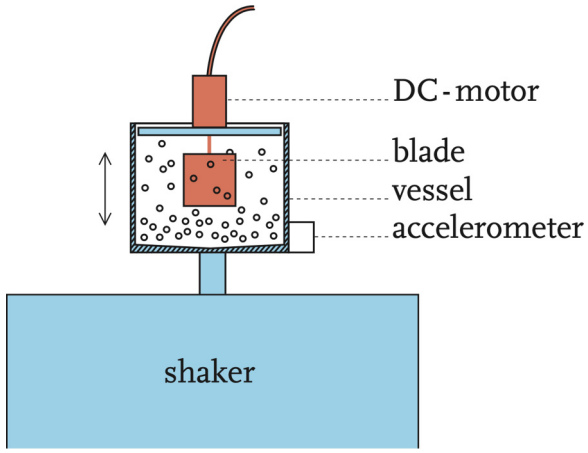

FIG. 1. The granular gas is excited in a cylindrical vessel by the vertical acceleration from an electromagnetic shaker. A small blade is fixed on the vertical shaft of a DC micromotor set on the immobile cover of the cell. Its rotation is caused by the random collisions with the gas.

II. EXPERIMENT

The experimental setup is composed of two identical granular gas systems. They play the role of two heat reservoirs, coupled to one another. Each consists of about 400 stainless steel beads (3 mm in diameter, 0.1 mg mass), steadily shaken vertically at a few grams and frequency 40 Hz, by an electromagnetic shaker. The beads are contained in 5-cm-diameter cylindrical cells (see Fig. 1). The probes are 2 cm × 2 cm × 0.2 mm steel blades, fixed on the vertical shafts of DC micromotors (Maxon, RE 10 118 386).

In this configuration, which respects the axial symmetry, the collisions with the gas particles make the blade rotate randomly like a one-dimensional (1D) Brownian object [2,23]. A key feature is that a DC motor can also operate symmetrically as a generator (dynamo). The voltage induced at the terminals, called electromotive force (EMF), is proportional to the angular velocity: $e(t) = \alpha\dot{\theta}(t)$ (Faraday's law of induction). The constant $\alpha \simeq 4.27 \times 10^{-3}$ V s/rad is a characteristic of the device. Conversely, it turns a current I into a torque, $\Gamma(t) = \alpha I(t)$ (Lorentz force), and therefore exchanges work with the gas. Note that the constant α is the same in both uses. Thanks to this dual function, the DC motor can impose a torque on the rotor imbedded in the gas and measure the velocity at the same time. It is the only probe used here, which performs measurements on the granular gas. The two probing motors are connected one another by a resistor R (see electrical diagram in Fig. 2).

The two NESS heat baths are therefore weakly coupled one another. The voltages $u_1(t)$ and $u_2(t)$ are recorded at the terminals of R by a NI-PXI 24-bit synchronous A/D converter.

Note that no external power is supplied to the motors: the collisions of the beads on blade 1 causing its rotation induces a voltage e_1. This voltage generates a current I through R into motor 2, causing rotation of blade 2. As a net result, some momentum is transferred from bath 1 to bath 2, and reversely.

We therefore have at hand an original setup to investigate the heat transport between two heat baths at different

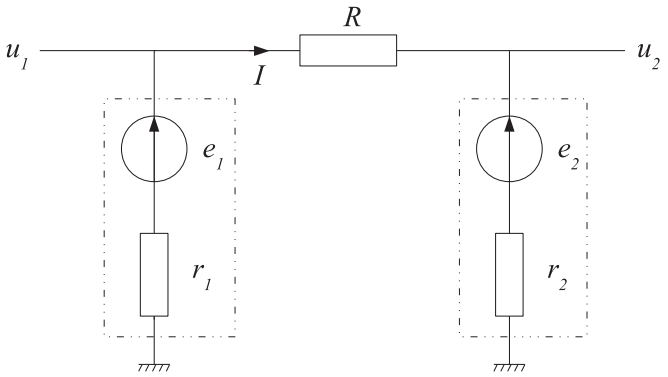

FIG. 2. The two motors, coupled to baths 1 and 2, are represented in dashed rectangles by ideal voltage sources of EMF, e_1 and e_2 (the instantaneous values of which are linked to the velocity of the rotors), and their internal resistances r_1 and r_2. The coupling resistor is R.

temperatures. One major specificity is that heat baths are in NESS instead of equilibrium states. In the last decade, many have worked to verify that the analogy holds, at least as far as stochastic thermodynamics features are concerned. Moreover, the design of the electromechanical coupling allows simple and reliable measurements of energy flux as well as temperatures.

III. HEAT FLUX AND TEMPERATURE MEASUREMENT

The voltages induced in each motor separately are simply

$$\begin{aligned} e_1 &= u_1 + r_1 I, \\ e_2 &= u_2 - r_2 I. \end{aligned} \tag{3}$$

The internal resistances of the motors are r_1 and r_2, and the inductances are negligible. The current, constant over the loop, is

$$I = \frac{1}{R_{\rm tot}}(e_1 - e_2) = \frac{1}{R}(u_1 - u_2). \tag{4}$$

The total resistance of the circuit is $R_{\rm tot} = R + r_1 + r_2$. The energy flux between 1 and 2 is the difference between the back-and-forth fluxes:

$$\begin{aligned} \phi(t) &\equiv (\dot\theta_1(t) - \dot\theta_2(t))\Gamma(t) \\ &= (e_1(t) - e_2(t))I(t). \end{aligned} \tag{5}$$

Noting that at any given moment, each device is virtually either generator or motor but never both at the same time, conservation of energy implies that the flow is

$$\phi(t) = \frac{1}{R_{\rm tot}}\big(e_1^2(t) - e_2^2(t)\big). \tag{6}$$

In addition, the voltages u_1 and u_2 are sufficient to express temperatures in both baths. Two approaches have been proposed to define and measure the effective temperature kT. Both rely on comparing the torque performed [current $I(t)$] and the velocity [EMF $e(t)$]. One is making use of the fluctuation theorem and the other of the fluctuation dissipation theorem (FDT), both theorems being invoked in a heuristic way. The relative distance between these two temperature

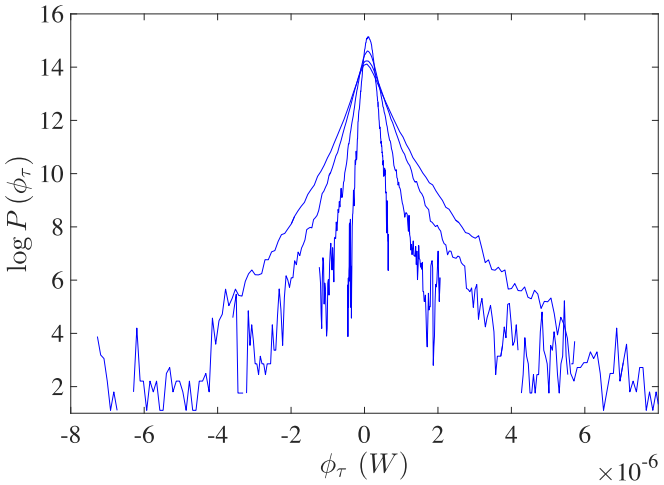

FIG. 3. Histograms of the coarse-grained heat flux ϕ_τ for several values of τ. (From the widest to the narrowest histograms: $\tau \simeq$ 50 ms, 100 ms, 300 ms, 1.2 s.) Here, the average flux is $\overline{\phi} \simeq 113$ nW, for $\Delta\beta \simeq 9.37 \times 10^4\,\mathrm{J}^{-1}$.

measurements is less than 10%. The temperature kT is linked to the kinetic energy of the rotor [3]:

$$kT_i = a + \tfrac{1}{2} bJ\overline{\dot\theta_i^2}. \tag{7}$$

J is the moment of inertia ($J \simeq 3.33 \times 10^{-8}\,\mathrm{kg\ m^2}$). The constants $a \simeq 4 \times 10^{-7}$ J and $b \simeq 2.5$ must be measured. The relation between the kinetic energy of a 1D free rotor in equilibrium with a thermostat, itself at equilibrium at temperature kT, would be $\frac{1}{2}J\overline{\dot\theta^2} = \frac{1}{2}kT$. Obviously, such equipartition cannot be assumed in a NESS thermostat. The value of the slope $b \simeq 2.5$ ($\gtrsim 2$) reflects the dissipative nature of the granular gas and the collisions between the beads and the blade. The constant a is the temperature that the gas must reach for the beads to get to the probe. The value $a \neq 0$ reflects the fact that the gas is stratified. The coefficients a and b depend on the properties of the granular gas itself, which is not the purpose of the present study. Finally, the temperature difference is simply, in electrical variables,

$$kT_1 - kT_2 = \frac{bJ}{2\alpha^2}\big(\overline{e_1^2} - \overline{e_2^2}\big). \tag{8}$$

The Fourier law for heat conduction is recovered:

$$\overline{\phi} = \frac{1}{R_{\rm tot}}\big(\overline{e_1^2} - \overline{e_2^2}\big) \tag{9}$$

$$= \frac{2\alpha^2}{bJR_{\rm tot}}(kT_1 - kT_2). \tag{10}$$

Note that this expression of the linear response is not exact in the sense that the coefficient b, reflecting the phenomenology of the granular gas, is to be measured.

Let us, from now on, focus on the instantaneous flux $\phi(t)$. It is directly calculated from the EMF $e_i(t)$ obtained from voltages at the terminals of R, as expressed by Eq. (6). This flux represents the difference between the heat flux given by bath 1 and that given by bath 2.

An example of a histogram, in Fig. 3, shows that the fluctuations of ϕ are indeed asymmetric and intermittent. The time

coarse grained $\phi_\tau(t)$ tends to be Gaussian for increasing τ, thanks to the central limit theorem. Note that the magnitude of the fluctuations can be of the same order but also much larger than the average energy flow, because, among the huge number of degrees of freedom of such macroscopic systems, only a very few are involved in this transport process. Note also that the mean flux can be of the order of 10^{-7} W, or even much smaller. In any case, it is very very little if compared to the power injected into the granular gas by the shakers ($\sim$10 W), attesting that the coupling is indeed very weak.

IV. TEST OF THE XFT IN THE NONDISSIPATIVE LIMIT

We have already shown that the heat flux satisfies Eq. (2), with a setup similar to this one [7]. However, the baths being dissipative, the hypothesis for the XFT proposed by Jarzynski and Wójcik are not fulfilled. Indeed, the slope μ of Eq. (2) was found to be quantitatively distinct from $\Delta\beta$, although of the same order. We explore here the following idea: vary the resistance R and compare the subsequent values of μ. Extrapolating $\frac{\mu}{\Delta\beta}$ versus $R_{\rm tot}$ gives the "nondissipative coupling limit" when $R_{\rm tot} \to 0$.

Previously, μ was measured thanks to the slope of the asymmetry function $\delta(\phi_\tau) = \frac{1}{\tau}\log\frac{P(\phi_\tau)}{P(-\phi_\tau)}$ versus ϕ_τ. The asymptotic values of the slope μ, in the large time limit $\tau \to \infty$, were compared to $\Delta\beta$. This protocol is difficult to implement in a stable manner. For instance, it is sensitive to the large range of conditions we address here (various R and ΔkT) and to the sample size. In the end, the uncertainties are difficult to control.

Here we have used another method to measure the same quantity. This method was found fruitful in another context [24], in the sense that it is more practical. It is strictly equivalent in the limit of large τ. It is based on the ratio of the two first moments of the flux:

$$\mu = \frac{\tau}{2}\frac{\overline{\Delta\phi_\tau^2}}{\overline{\phi_\tau}}, \quad \text{for } \tau \to \infty, \tag{11}$$

where $\overline{\phi_\tau}$ is the mean, and $\overline{\Delta\phi_\tau^2}$ is the variance of the flux. This alternative method, efficient and obviously much easier in practice, is valid even for variables like ϕ_τ, which are Gaussian only for the largest τ. Convergence is easier because it involves low order moments only, which counts at large τ (see Fig. 4). Also, the ratio 11 can be calculated even though negative values of ϕ_τ are absent. It is known that the relaxation at finite time is not universal [25,26]. Now, as we are only interested in the $\tau \to \infty$ asymptotic value of μ, what is the most precise and reliable way to evaluate it? A robust protocol must be defined, unique to all conditions of interest here: all temperature gradients ΔkT, at various R. In the large τ limit, we found it convenient to use an exponential fitting to obtain the value of the asymptote in a stable and reproducible way. The ratio given in Eq. (11), $\frac{\tau}{2}\frac{\overline{\Delta\phi_\tau^2}}{\overline{\phi_\tau}}$, is calculated for various times τ for a large number of samples and plotted versus τ in Fig. 5, together with an exponential best fit: $\mu + c\,\exp(-\tau/\tau^*)$.

The agreement, although not perfect, is acceptable for any configuration of interest here. Averaging the limit value obtained from this fitting over dozens of time series gives a measure of the slope μ. The rms gives an estimate of the uncertainties.

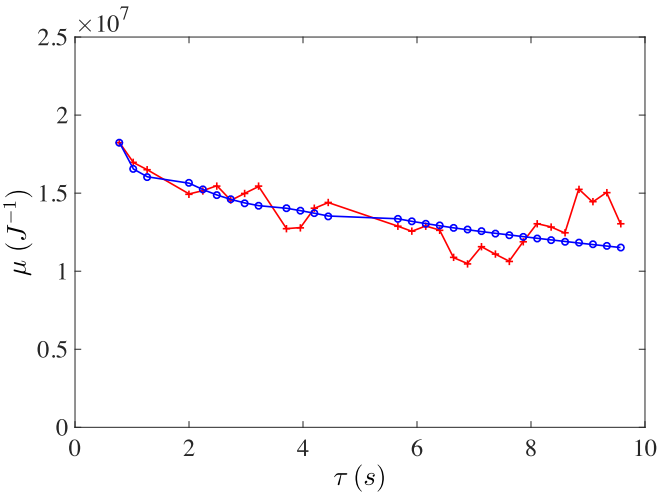

FIG. 4. The slope of the asymmetry function for a 1-h-time sample, obtained from Eq. (11), is plotted for various times τ ($\circ$) during relaxation. The red curve (+) shows the analysis of the same sample by the best linear fit of the asymmetry function. Here $R = 100.23\,\Omega$, and $\Delta\beta \simeq 9.37 \times 10^4\,\mathrm{J}^{-1}$.

Effective temperatures kT_i in both thermostats are calculated thanks to the variances of the EMF, $e_i(t)$, and Eq. (7), that is to say, using the coefficient b obtained in [3]. As mentioned in Lecomte and Naert [7], the relation between μ and $\Delta\beta$ is linear for the value $R = 22\,\Omega$. For self-consistency of the paper, the main figure from Lecomte and Naert is reproduced in Fig. 6. It was noted at the time that the slope was not 1, in contrast to the XFT. Acknowledging this proportionality, we performed new measurements for different resistances R,

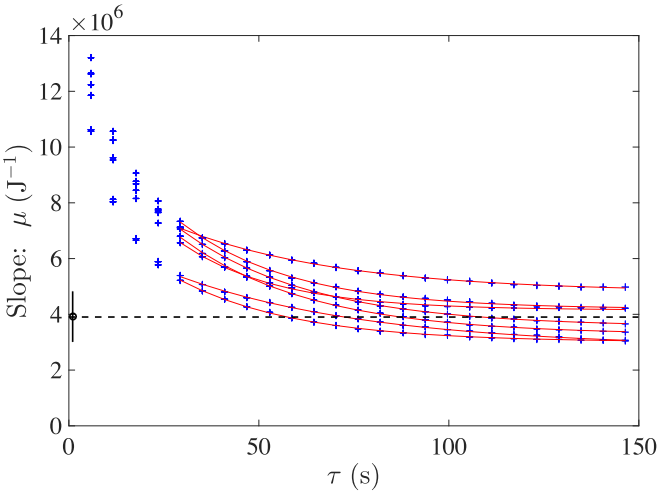

FIG. 5. The slope of the asymmetry function for a few time series, calculated thanks to Eq. (11), is plotted for various time lags τ (+). The red curves show best exponential fits. The dashed black line represents the average of these limits at large τ over dozens of time series. The rms of μ is in black. Here $R = 23.28\,\Omega$, while $\Delta\beta \simeq 1.5 \times 10^5\,\mathrm{J}^{-1}$.

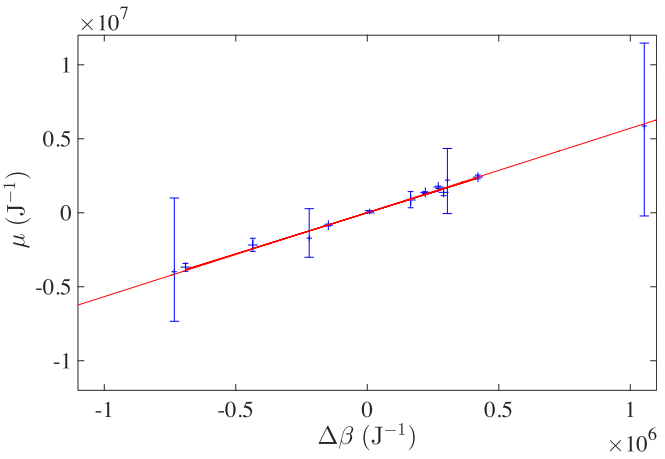

FIG. 6. The relation between μ and $\Delta\beta$ is linear for $R = 22\,\Omega$, and the slope is $\frac{\mu}{\Delta\beta} \simeq 5.69$. This figure is taken from Ref. [7].

only for a few values of temperature difference to ascertain the variation of the slope.

Several measurements of μ are plotted against $\Delta\beta$, superimposed in Fig. 7. These results show that the proportionality coefficient between μ and $\Delta\beta$ decreases monotonously with R.

To be fair, one must consider the total resistance in the loop in order to account for the total dissipation in the coupling, $R_{\rm tot} = R + r_1 + r_2$. The dependance of $\frac{\mu}{\Delta\beta}$ in $R_{\rm tot}$ is presented in Fig. 8. In order to extrapolate to $R_{\rm tot} = 0$, a polynomial fitting is performed (second order is sufficient). It leads to the slope $\frac{\mu}{\Delta\beta} \simeq 0.85$ in the nondissipative limit. This value is compatible with unity, as expected by the XFT. Here is the main result of this study.

At this point, a discussion of the uncertainties is pivotal. Some of the errors in μ are due to the exponential fitting process presented above to determine the asymptote, and some to statistic limitations. Additional uncertainty arises with regard to $\Delta\beta$ because of the 10% error in the coefficient b, a consequence of the relative uncertainty of the same order regarding kT, as mentioned above. Minor errors come from the drift in room temperature, like night and day variations (inducing variations of $\sim$1% at most on r_i). The error bars on $R_{\rm tot}$ are imperceptible, see Fig. 8. Note that the increase of the error bars with R is due to the current decrease, deteriorating the signal-to-noise ratio. All this leads to an uncertainty on the ratio $\frac{\mu}{\Delta\beta}$, overall estimated to be about 1 at most. In the end, it is a fraction of a percent in relative value, which is satisfactory.

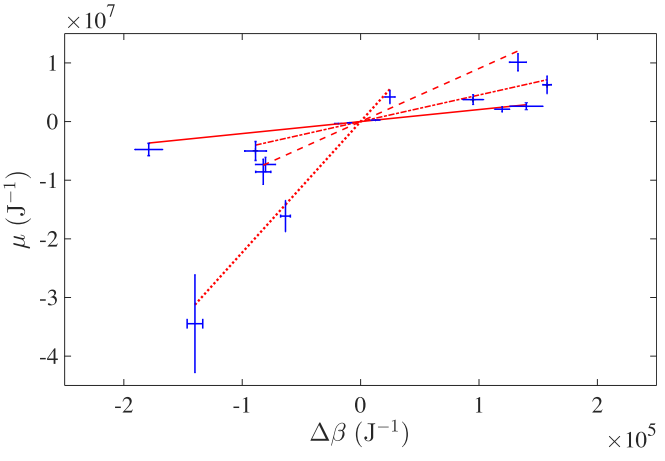

FIG. 7. The slope μ is plotted against $\Delta\beta$ for a few values of the coupling resistance $R = 23.27\,\Omega$ (solid), 100.23 Ω (dash-dot), 242.6 Ω (dash), and 617.4 Ω (dot). The red lines represent in each case the best linear fits through zero.

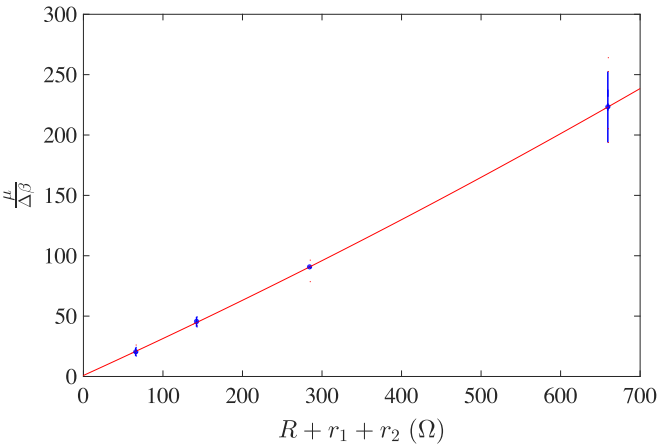

FIG. 8. The ratio $\frac{\mu}{\Delta\beta}$ is plotted against the resistance $R_{\rm tot}$. A second-order polynomial fitting is performed $y = p_1 x^2 + p_2 x + p_3$ (in red). The coefficients obtained are $p_1 \simeq 5.63 \times 10^{-5}$, $p_2 \simeq 0.30$, $p_3 \simeq 0.85$. In the zero-resistance limit, $\frac{\gamma}{\Delta\beta} \to p_3 \simeq 0.85$.

V. DISCUSSION AND CONCLUSION

We have presented a continuation, until concluding, of the preceding work of Lecomte and Naert in 2014 on the transport of heat between two NESS thermostats maintained at different effective temperatures kT_i. Two identical centimeter-size 1D-Brownian mobiles, fastened on electric micromotors, are immersed in granular gas heat baths. The motors are electrically linked to one another by a resistance R, insuring a weak coupling between the baths. Electrical measurements at the terminals of R give access to the flux $\phi(t)$ and the temperature in each bath, kT_i. In the present study, the coupling is varied by changing R. For each value the ratios of the variance over the mean flux are calculated. This is equivalent to the slope of the asymmetry function for several temperature differences. We show experimentally that, extrapolating to the nondissipative coupling limit ($R \to 0$), the fluctuations of the flux are compatible with the exchange fluctuation theorem (XFT) proposed by Jarzynski and Wójcik (2004) in the large time limit. It is written like Eq. (2), the free parameter μ being here nothing but the inverse temperature difference: $\Delta\beta = \frac{1}{kT_1} - \frac{1}{kT_2}$. Whereas the Fourier law for heat transfer links the mean flux and temperature gradient, the XFT expresses the asymmetry of the fluctuations, among nonequilibrium as well as equilibrium finite size subsets.

There are several interesting aspects to the experimental observation of the XFT in such a context, where it is unexpected. A first question that requires careful reflection is where nonequilibrium actually stands. The XFT, like other

FT, applies to such an out-of-equilibrium situation where heat flows between two systems. It is intrinsically a nonequilibrium feature. Consequently, having the flux between two baths coupled verifying XFT as well as Fourier law looks unsurprising in the end. The concern is more acute about the dissipative nature of the granular gas itself. (See a questioning of the FT in this context in [27].) The NESS of the granular gas results from the balance between work injection and heat dissipation. Once in a steady state of fluctuations, the Brownian rotor experiences kicks, but one cannot know whether this random forcing results from an equilibrium state or merely a NESS. Mathematically, the coupling with the bath is represented by a random forcing term in the equation of motion of the rotor. It has no signature of the irreversibility of the underlying work-to-heat conversion process. Another question concerns the effective temperature kT that characterizes the agitation of the beads. The verification of the laws of heat transport in a temperature gradient, for the average as well as fluctuations, confirms once more that kT behaves the same way as an equilibrium temperature. This second observation looks even more striking, but it is just another aspect of the previous one: NESS or equilibrium state heat baths are not the same. Indeed, they just behave the same from the point of view of applying stochastic thermodynamics on the rotor. This is obviously not true for the motion of the beads in the granular gas!

Intriguing deductions are starting to emerge from these results. First of all, the field of application of stochastic thermodynamics appears not to be limited to the molecular scale. Some open questions on macroscopic-scale phenomena are not addressed by statistical physics because they are out of equilibrium, that is, dissipative and spatially extended systems, such as those of interest in nonlinear physics. Yet it seems possible to invoke the theoretical arsenal of stochastic thermodynamics as a wedge in long-lasting problems such as hydrodynamic turbulence, wave turbulence, rapid fracture in solids, granular matter, etc.

ACKNOWLEDGMENTS

We are grateful to S. Aumaître, C. Crauste, A. Archambault, A. Steinberger, and J.-P. Zaygel for many discussions and suggestions in the course of the experiments, and also to J.-C. Géminard, M. Adda-Bedia, and C. Jarzynski for corrections and suggestions on the manuscript.

[1] I. Goldhirsch, Powder Technol. **182**, 130 (2008).
[2] A. Naert, Europhys. Lett. **97**, 20010 (2012).
[3] J.-Y. Chastaing, J.-C. Géminard, and A. Naert, J. Stat. Mech. (2017) 073212.
[4] I. Goldhirsch, Annu. Rev. Fluid Mech. **35**, 267 (2003).
[5] N. V. Brilliantov and T. Pöschel, *Kinetic Theory of Granular Gases* (Oxford University Press, England, 2004).
[6] Y. Oono and M. Paniconi, Prog. Theor. Phys. Suppl. **130**, 29 (1998).
[7] C.-É. Lecomte and A. Naert, J. Stat. Mech. (2014) P11004.
[8] D. J. Evans, E. G. D. Cohen, and G. P. Morriss, Phys. Rev. Lett. **71**, 2401 (1993).
[9] G. Gallavotti and E. G. D. Cohen, Phys. Rev. Lett. **74**, 2694 (1995).
[10] J. Kurchan, J. Phys. A: Math. Gen. **31**, 3719 (1998).
[11] J. L. Lebowitz and H. Spohn, J. Stat. Phys. **95**, 333 (1999).
[12] U. Seifert, Rep. Prog. Phys. **75**, 126001 (2012).
[13] C. Jarzynski, Annu. Rev. Condens. Matter Phys. **2**, 329 (2011).
[14] S. Ciliberto, Phys. Rev. X **7**, 021051 (2017).
[15] S. Ciliberto, C. R. Phys. **20**, 529 (2019); Prizes of the French Academy of Sciences 2018 / Prix 2018 de l'Académie des sciences, J. Villain, *ibid.* **20**, 503 (2019).
[16] S. Ciliberto and C. Laroche, J. Phys. IV (France) **08**, 215 (1998).
[17] R. Kubo, M. Toda, and N. Hashitsume, *Statistical Physics II, Nonequilibrium Statistical Mechanics*, Springer Series in Solid-State Sciences (Springer, New York, 1985).
[18] C. Jarzynski and D. K. Wójcik, Phys. Rev. Lett. **92**, 230602 (2004).
[19] A. Gomez-Marin and J. M. Sancho, Phys. Rev. E **73**, 045101(R) (2006).
[20] S. Ciliberto, A. Imparato, A. Naert, and M. Tanase, Phys. Rev. Lett. **110**, 180601 (2013).
[21] A. Bérut, A. Imparato, A. Petrosyan, and S. Ciliberto, Phys. Rev. Lett. **116**, 068301 (2016).
[22] K. Kanazawa, T. Sagawa, and H. Hayakawa, Phys. Rev. E **87**, 052124 (2013).
[23] J. Monsel, B. Pascal, J.-Y. Chastaing, J.-C. Géminard, and A. Naert (to be published).
[24] B. Apffel, A. Naert, and S. Aumaître, J. Stat. Mech. (2019) 013209.
[25] S. Ciliberto, S. Joubaud, and A. Petrosian, J. Stat. Mech. (2010) P12003.
[26] S. Joubaud, N. B. Garnier, and S. Ciliberto, J. Stat. Mech. (2007) P09018.
[27] P. Visco, A. Puglisi, A. Barrat, E. Trizac, and F. van Wijland, Europhys. Lett. **72**, 55 (2005).